The use of a digital twin to reconfigure a nonlinear internal model controller

Conference Paper · September 2022

CITATIONS
0

READS
25

2 authors, including:

Yoav Vered
University of Southampton
16 PUBLICATIONS **24** CITATIONS

SEE PROFILE

The use of a digital twin to reconfigure a nonlinear internal model controller

Y. Vered, S. J. Elliott
University of Southampton, Institute of Sound and Vibration Research,
Southampton, SO17 1BJ, United Kingdom
e-mail: **v.yoav@soton.ac.uk**

Preprint
Published as part of the ISMA-USD 2022 conference proceedings
http://past.isma-isaac.be/downloads/isma2022/proceedings/Contribution_159_proceeding_3.pdf

Abstract
A reconfigurable feedback controller based on a digital twin is illustrated using simulations of a system with a time-varying nonlinear backlash. The control system consists of a motor driving the position of a flexible structure through a lead screw subject to backlash, whose gap angle changes over time. An internal model control (IMC) approach is utilised as the feedback path to increase the linear controller robustness. When a backlash is considered in the model, it is shown that although the linear IMC remain asymptotically stable, its performance deteriorates. A nonlinear IMC (NIMC) approach improves the closed-loop system's transient behaviour. When the backlash model used in the NIMC is exact, the NIMC can follow the reference model. However, residual vibrations are observed if the backlash model is not estimated precisely. A digital twin of the system is used to estimate the backlash gap angle and to re-design the backlash model for the NIMC via asynchronous communication, thus ensuring the stability of the feedback system.

1 Introduction

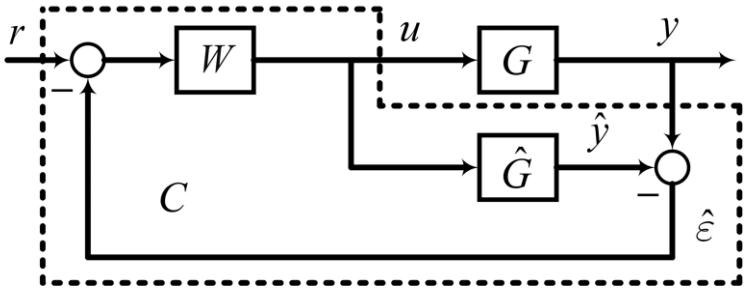

Figure 1: Block diagram of a feedback controller implemented using internal model control (IMC). The architecture of the complete feedback controller, C, is shown between the dashed line. G detnotes the dynamical plant, $\hat{G}$ its model, W the prefilter. r and y are the reference and output signals, respectively, u the control signal, $\hat{y}$ the predicted output, and $\hat{\varepsilon}$ the prediction error.

Internal model control (IMC) [1]–[3], represented by the block diagram in Figure 1, is a well-established concept for the design of feedback controllers for internally stable systems [2]. The advantage of using an IMC for the reference tracking or position control problems is in the fact that when the plant model is accurate, so that $\hat{G} = G$, an open-loop feedforward filter can be designed, which in general is more straightforward than designing a feedback controller. However, unlike the feedforward control, the IMC can then be used to attenuate the effect of input and output disturbances. Also, based on the small-gain theorem

it is easy to design a filter that ensure the closed-loop stability as long as the modeling error can be bounded [1].

Nonlinear IMC (NIMC) have also been discussed in the literature [4], and they can be combined in the adaptive control, where the internal model's parameters and the prefilter are being estimated simultaneously in real-time [5], [6]. However, such approaches result in a complex-structure controller whose implementation is not straightforward.

The novelty of the current work is to reconfigure the NIMC based on a digital twin of the system [7]. The digital twin defined here is a fusion of physical-based [8] and data-informed [9] models that can be realised on a remote server. The use of a digital twin gives rise to a simple-structure local NIMC and, at the same time, enables the use of nonlinear identification methods. Although different approaches may be already in use, where a physical model is being updated based on measured data [10], [11], followed by a design of a feedback controller [12], [13]. Most often, the model estimation and the controller design are performed by several experts. However, in the approach proposed here, the reconfiguration process is done automatically by pre-determine the controller's architecture and utilising the digital twin.

The digital twin reconfigurable NIMC idea is illustrated here based on a mechanical position control mechanism with a time-varying backlash. Initially, an IMC is designed to stabilise the otherwise not stable loop and obtain desired performance criteria. The nominal linear models of the system are used at this stage, allowing the exploitation of well understood linear controller design methods and ideas [12]. Then a time-varying backlash is introduced between the actuator and the flexible structure being controlled. Its effect is minimised by updating the previously designed controller to include a backlash model, which is then tuned using a digital twin to ensure that the performance objectives are kept.

Backlash is inherent to any mechanical motion transmission mechanism and can be modelled using a clearance, or a gap, between different parts of the mechanism [14]. Most often, passive solutions are used to minimize the backlash effects, an example is an anti-backlash nut that aims to reduce the clearance with a preloaded spring. However, a certain amount of play will always remain between different parts of the mechanism, and it is most likely to grow in time due to wear and tear effects. Active control of backlash was also previously considered [15]. But, when aimed at estimating the backlash parameters as part of the loop, such solutions result in a very complex controller, for example, see [16].

Here, based on a simulative case study, it is shown that the digital twin can be used to reconfigure a NIMC based controller, to maintain performance even for extremely rapid-growing backlash. The nonlinear optimisation performed using the digital twin allows for a relatively simple controller design, which can be combined in the future with other nonlinearities or time-varying parameters. In addition, the prediction error computed as part of the NIMC can be used to derive a novelty index [17] and consequently formulate a decision test of when to employ the digital twin and reconfigure the backlash model.

The paper is organized as follows. The linear models of the systems and the design of the linear IMC are presented in Sections 2.1 and 2.2, respectively. The nonlinear backlash model is introduced in section 3.1, followed by a numerical simulation of the linear IMC closed-loop to time-varying backlash discussed in section 3.2, and the same simulation for a NIMC closed-loop with a constant backlash estimation. The digital twin and backlash estimation method are presented, and the performance of the reconfigurable NIMC is evaluated in Section 4.1. A novel index-based decision test is described and simulated in Section 4.2. Finally, conclusions are summarised in section 5

2 Linear Modelling

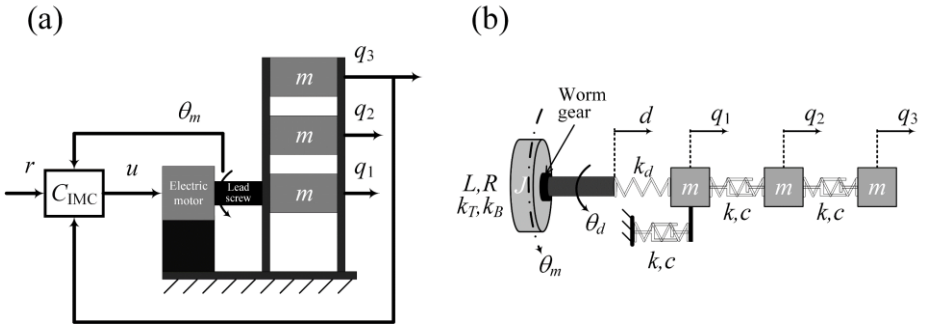

Figure 2: The model of the simulated three DOF system with an IMC based feedback controller (a), and the electromechanics system's lumped element model (b).

In this paper, a feedback controller is designed to control the position of a three DOF structure, similar to the one considered in [18], as shown in Figure 2(a). The bottom mass of the structure is connected to a dc electromechanics motor via a lead screw. A simplified dynamic system model is derived using lumped elements, as shown in Figure 2(b). The dc motor electrical model parameters are its inductance, L, and resistance, R, it is modelled as a lumped inertia, J, the two motor's coefficients, k_T and k_B are the torque and back-emf gains, and the motor angular velocity and position are denoted ω_m and θ_m, respectively. The three DOF structure is modelled as three equal lumped masses, each of mass m, connected in series via linear springs, k, and linear dampers, c. The lead screw is connected to the motor via a worm gear with a 1:1 gear ratio. Its angular position is denoted as θ_d and its elongation (from rest) is denoted as d such that $d = p\theta_d$, where p is the pitch of the lead screw. The absolute position of each of the structure's platforms are denoted q_i ($i = 1,2,3$). However, the worm gear is likely to developing backlash, and so the motor's angle, θ_m, does not necessarily equal that of the lead screw, θ_d.

2.1 Linear models derivation

In the derivation of the nominal linear models, the following assumptions are used: The inertial loading of the structure is negligible compared to the motor's torque; The lead screw is infinitely rigid, i.e., $k_d \to \infty$; The worm gear does not have any backlash, i.e., $\theta_d = \theta_m$.

Under these assumptions, the electromechanics-dynamical model of the motor is given by:

$$L\dot{I}_m + RI_m = u - V_b, \tag{1}$$

$$J\dot{\omega}_m = T_m, \tag{2}$$

where $I_m, u,$ and V_b denote the motor's electrical current, input voltage, and back-emf, respectively. T_m denote the mechanical torque that is proportional to the electrical current

$$T_m = k_T I_m. \tag{3}$$

Also, the back-emf is proportional to the motor's angular velocity

$$V_b = k_B \omega_m. \tag{4}$$

Taking the Laplace transformation with zero initial conditions of Eq. (1) – (4) and performing algebraic manipulations results in the following relation:

$$\omega_m(s) = \frac{k_T}{JLs^2 + JRs + k_B k_T} u(s). \tag{5}$$

Defining the transfer function between the input voltage to the angular position as $G_1(s)$, it follows that:

$$G_1(s) = \frac{1}{s} \frac{k_T}{JLs^2 + JRs + k_B k_T} \tag{6}$$

The free three DOF structure's equations of motion (EOM) can be written using matrix notation as:

$$\begin{bmatrix} m & 0 & 0 \\ 0 & m & 0 \\ 0 & 0 & m \end{bmatrix}\begin{bmatrix} \ddot{q}_1 \\ \ddot{q}_2 \\ \ddot{q}_3 \end{bmatrix}+\begin{bmatrix} 2c & -c & 0 \\ -c & 2c & -c \\ 0 & -c & c \end{bmatrix}\begin{bmatrix} \dot{q}_1 \\ \dot{q}_2 \\ \dot{q}_3 \end{bmatrix}+\begin{bmatrix} 2k & -k & 0 \\ -k & 2k & -k \\ 0 & -k & k \end{bmatrix}\begin{bmatrix} q_1 \\ q_2 \\ q_3 \end{bmatrix}=\begin{bmatrix} 0 \\ 0 \\ 0 \end{bmatrix}. \quad (7)$$

Since we assumed that the lead screw is infinitely rigid, it follows that $q_1 = d = p\theta_d$. After substituting q_1 into the EOM of Eq. (7), and reorganizing, the following set of equations is obtained:

$$\begin{bmatrix} m & 0 \\ 0 & m \end{bmatrix}\begin{bmatrix} \ddot{q}_2 \\ \ddot{q}_3 \end{bmatrix}+\begin{bmatrix} 2c & -c \\ -c & c \end{bmatrix}\begin{bmatrix} \dot{q}_2 \\ \dot{q}_3 \end{bmatrix}+\begin{bmatrix} 2k & -k \\ -k & k \end{bmatrix}\begin{bmatrix} q_2 \\ q_3 \end{bmatrix}=\begin{bmatrix} c \\ 0 \end{bmatrix}p\dot{\theta}_d+\begin{bmatrix} k \\ 0 \end{bmatrix}p\theta_d. \quad (8)$$

The transfer function from θ_d to q_3, defined as $G_2(s)$, is obtained by taking the Laplace transformation with zero initial conditions of Eq. (8), and solving the linear algebraic system such that:

$$G_2(s) = \frac{c^2s^2+2cks+k^2}{m^2s^4+3cms^3+(c^2+3km)s^2+2cks+k^2}p \quad (9)$$

The numerical values used throughout the rest of the paper simulations are given in Table 1

Table 1: Physical properties and values used in the numerical simulations

Symbol	Value, units	Symbol	Value, units	Symbol	Value, units
$\boldsymbol{m}$	5.2, kg	$\boldsymbol{J}$	$5 \cdot 10^{-6}$, kg·m²	$\boldsymbol{p}$	$2/2\pi$, mm/rad
$\boldsymbol{k}$	$1 \cdot 10^{4}$, N/m	$\boldsymbol{L}$	$1 \cdot 10^{-3}$, H	$\boldsymbol{k_T}$	0.8, (N·m)/A
$\boldsymbol{c}$	36.9, N/(m·s)	$\boldsymbol{R}$	12, ohm	$\boldsymbol{k_B}$	0.1, V/(m/s)

2.2 Linear controller design

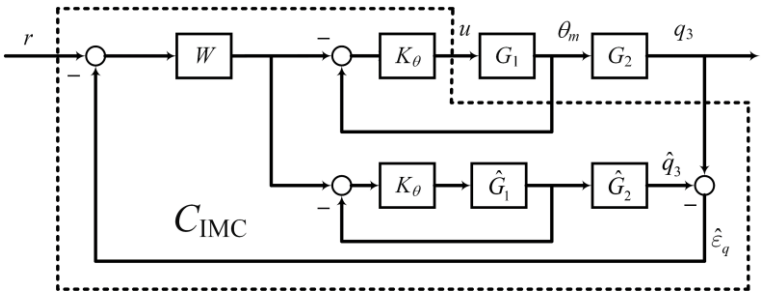

Figure 3: Block diagram showing the architecture of the controller designed based on IMC. G_1 and G_2 are the LTI systems defined in Eq. (6) and (9), W denotes the prefilter to be designed, and K_θ the proportional feedback gain tuned to stabilize the motor's dynamics. $\hat{G}_1, \hat{G}_2, \hat{q}_3$, and $\hat{\varepsilon}_q$ denote the sampled-data models of the motor and three DOF structure, the predicted output, and the prediction error, respectively. Once again the complete feedback controller is shown inside the dashed lines.

A digital IMC based controller is proposed, as shown in Figure 3. The controller inputs are the reference signal, the measured motor's angle, and the measured top platform position, and its output is the voltage input of the motor. When the internal model of the sampled-data systems is exact, the feedback is cancelled, and the controller is a feedforward controller. Thus, the IMC configuration cannot stabilise unstable poles of the system. In our case, the electrical motor contains an integrator, and therefore, an internal loop is introduced around it to ensure that the open-loop transfer function is stable. In the following sections, the stabilisation of the electrical motor is achieved via a proportional feedback gain tuned to achieve a settling time of 30msec. The feedback gain was, therefore, tuned to be:

$$K_\theta = 15 \quad (10)$$

The motor's input is no longer the electric voltage when using the proportional feedback controller. Instead, it is a reference angle, which the feedback controller aims to follow. The open-loop transfer function, to be used in the IMC design, from the input reference angle to the top mass position denoted as G_{ol}, is given by:

$$G_{ol}(s) = G_\theta(s)G_2(s). \tag{11}$$

where G_θ denotes the equivalent transfer function of the inner feedback loop:

$$G_\theta(s) = K_\theta G_1(s)/\big(1 + K_\theta G_1(s)\big), \tag{12}$$

Since now the open-loop transfer function is stable, if a constant input is used, the steady state top mass position is given by the final value theorem as:

$$q_3(t \to \infty) \to W(s \to 0)G_{ol}(s \to 0) = W(0)G_\theta(0)G_2(0) \tag{13}$$

It follows that $G_\theta(0) = 1$, which can be shown by substituting Eq. (6) and (10) into (12) and taking the limit $s \to 0$. Similarly, substituting $s = 0$ in equation (9) results in $G_2(0) = p$.

Therefore, the prefilter, W, is normalised by the lead screw's pitch, such that:

$$W(s) = \widetilde{W}(s)/p \tag{14}$$

For a chosen $\widetilde{W}$ that holds, $\widetilde{W}(0) = 1$.

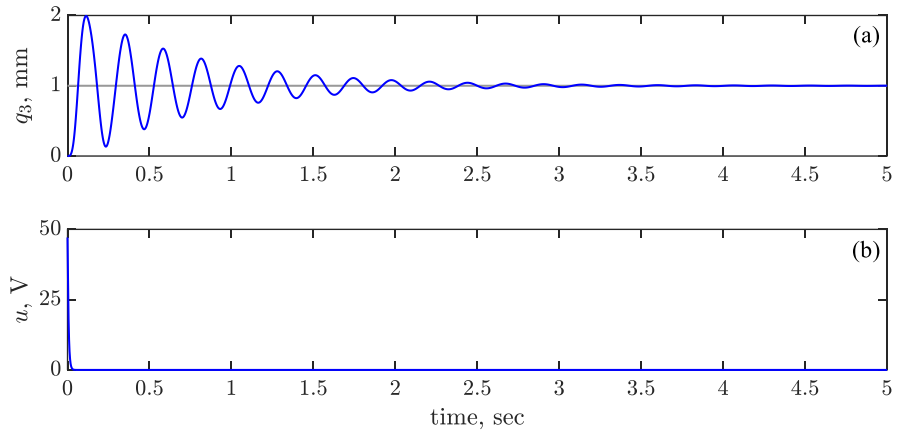

Figure 4: The top platform position (a) and the motor's input voltage (b) response to a step input in the reference signal for the linear system with the internal proportional feedback loop, no dynamical prefiltering and a perfect sampled-data model.

Figure 4(a) shows the 1mm step responses for a perfect sampled-data model with no dynamical prefiltering, i.e., $\widetilde{W}(s) = 1$. Figure 4(b) shows the control signal, that is, the motor's input voltage, needed for the manoeuvre. It is noted that the overshoot is almost 100%, the settling time is about 3.5 seconds, and the required maximal input voltage is 47 Volts. Therefore, it is desirable to design a dynamical prefilter, $\widetilde{W}$, to obtained better transient and reduce the required input voltage (and power) supplied to the motor.

2.2.1 Prefilter design – Model reference approach

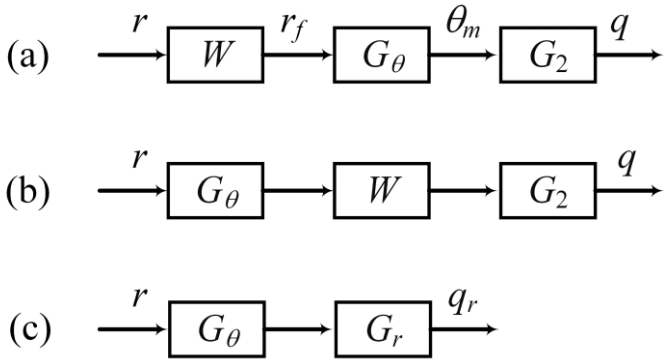

Figure 5: The open-loop with a prefilter block diagram (a), equivalent model of the open-loop with a prefilter for LTI W and G_2 (b), and the desired filtered plant structure (c).

To improve the transient performance of the system, a dynamical prefilter, W, is used. For LTI systems, the order can be swapped between G_θ and W as shown in Figure 5(b) compared to Figure 5(a). Figure 5(c) is then obtained by denoting the series interconnection of W and G_2 as G_r. If G_r has a relative rank equal or larger to that of G_2, and it contains all the non-minimum-phase zeros of G_2, a stable W can be designed $W = G_2^{-1}G_r$. However, in this work a different approach is taken. Since only one dominant mode is seen in the response of Figure 4(a), we wish to filter only that dominant mode. The rational transfer function of Eq. (9) can be described with a balanced truncated reduced-order model [19] as a second-order system with a relative degree of 0. Therefore, neglecting the fast dynamic and choosing G_r as a first-order filter with a time constant τ_r, to minimize the effect of the fast modes; $\widetilde{W}$ can be designed as:

$$\widetilde{W} = \frac{1}{\tau_r s+1} G_d^{-1} \tag{15}$$

where G_d is the part of the balanced truncated reduced-order model of the normalized transfer function $G_2/G_2(0)$.

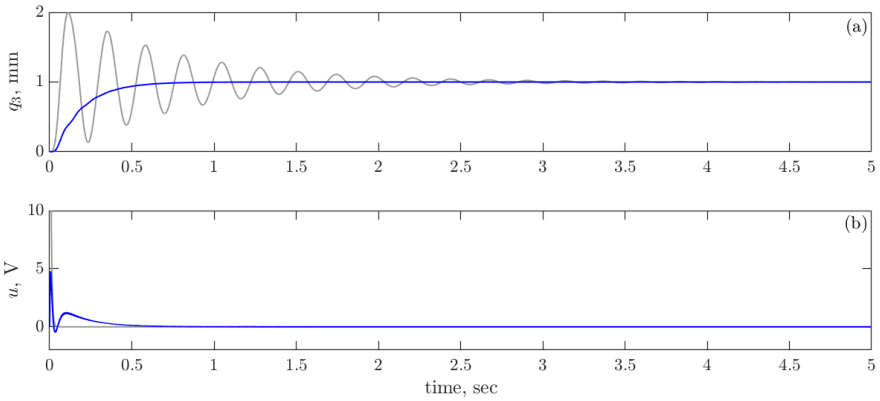

Figure 6: The top platform position (a) and the motor's input voltage (b) response to a step input in the reference signal for the linear system with the internal proportional feedback loop and dynamical prefiltering based on the balanced truncated reduced model of G_2, and a perfect sampled-data model

Figure 6 shows the results of the step input when using the dynamical prefiltered design based on the balanced truncated reduced-order model of G_2, with a τ_r chosen as $1/6$ to approximate a settling time of 0.8 seconds. As shown in Figure 6(a), the desired settling time is obtained, and the overshoot is eliminated. The effect of the higher-order dynamics can be noted by the fact that the derivative at $t = 0$ is not zero. The required input voltage peak, Figure 6(b), is now below 5 Volts.

3 Nonlinear modelling

So far, we have designed the IMC controller based on nominal linear models of the system. In the current section, a nonlinear backlash is introduced between the motor and the three DOF structure, and the combined effect of the sampled-data system and nonlinear time-varying backlash are simulated.

3.1 Backlash models

The worm gear's backlash mechanism is modelled as a dead zone for the angular velocity. Each time the rotation direction changes, a new dead zone of a given backlash gap angle begins.

The backlash nonlinear operator is given by

$$\omega_d = g(z,\sigma)\omega_m \tag{16}$$

where

$$g(z,\sigma) = \begin{cases} 1 & (\sigma > 0 \;\&z \geq \theta_b)|(\sigma < 0 \;\&z \leq -\theta_b\,) \\ 0 & \text{Otherwise} \end{cases} \tag{17}$$

In the model $z = \theta_m - \theta_d$ denotes the difference between the motor and lead screw angles, $\sigma = \text{sign}(\dot{\omega}_m)$ denotes the motor's direction of rotation, and θ_b the backlash gap angle, or half-width.

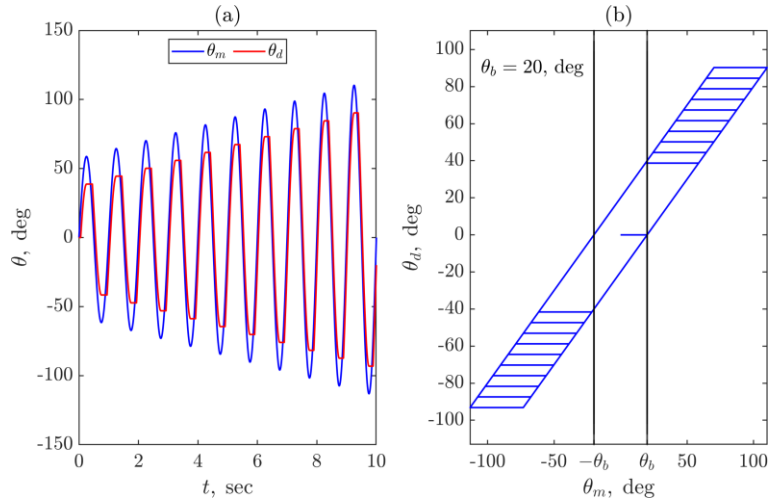

Figure 7: Input and output of the backlash model for a sinusoidal input with a growing amplitude versus time (a) and in state-space (b).

Figure 7 shows the output of the backlash for $\theta_b = 20$ deg, and a sinusoidal input with a growing amplitude:

$$\theta_m(t) = (1 + t/10)\sin(2\pi t).$$

Figure 7 shows the effect of the velocity dead-zone on the lead screw's angle. Each time the direction of rotation changes, θ_d remains constant until the backlash is transverse. Then, θ_d follows θ_m with a constant lag of $2\theta_b$. The former is best seen in Figure 7(a), while the latter in Figure 7(b).

3.2 Time-varying backlash simulation

A Simulink simulation with a time-varying backlash model was used to simulate the wear and tear effect on the digital IMC feedback system. The backlash gap angle is varied between 0 to 100 degrees based on a pre-designed S-curve profile. Thus, mimicking a highly accelerated wear and tear effect. The sampling time is set to $T_s = 1$msec, which represents a sampling frequency of $F_s = 1000$Hz. In the simulation a digital

controller is realised, using the zero-order hold assumption to derive the sampled-data models of the different systems used in the controller ($W, \hat{G}_1, \hat{G}_2$). The reference signal was chosen to be a unit (1mm) square wave with a period of 40 seconds, and the simulation run-time was chosen to be 200 seconds.

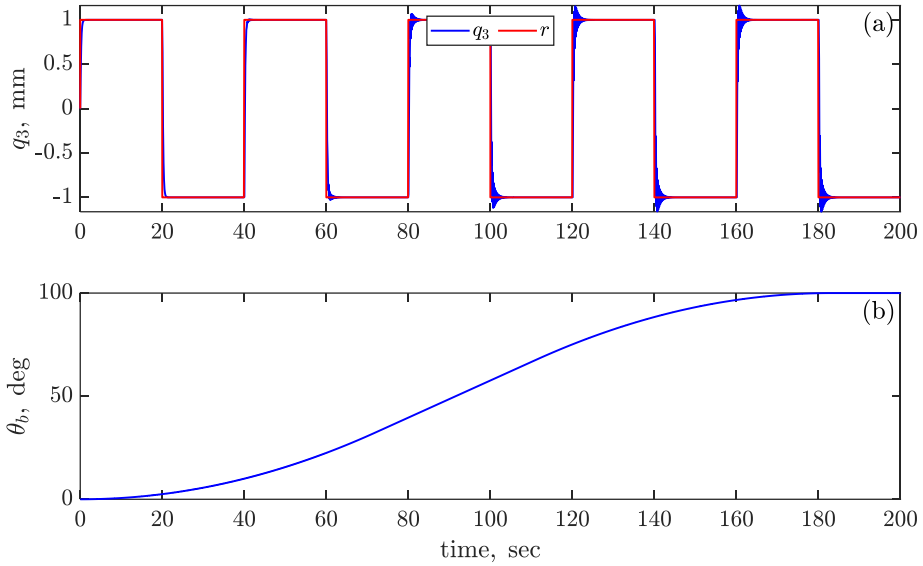

Figure 8: The time-varying backlash simulation results with the linear IMC controller. The reference and output signals (a) and the backlash gap angle (b) versus time.

Figure 8 shows the simulation results for the S-curve varying backlash gap angle of Figure 8(b). Based on Figure 8(a), it is noted that the sampling has a negligible effect on the feedback. Consequently, when the backlash is small (time<60 seconds), the transient behaviour is similar to the designed one shown in Figure 6(a), with no overshoot and a settling time of less than a second. However, when the backlash gap angle becomes larger, a significant overshoot is observed, and the transient response is composed of decaying oscillations. Therefore, to ensure that the transient behaviour is kept for a considerable backlash, a model of the backlash will be added to the IMC controller, rendering it nonlinear.

3.3 Nonlinear controller

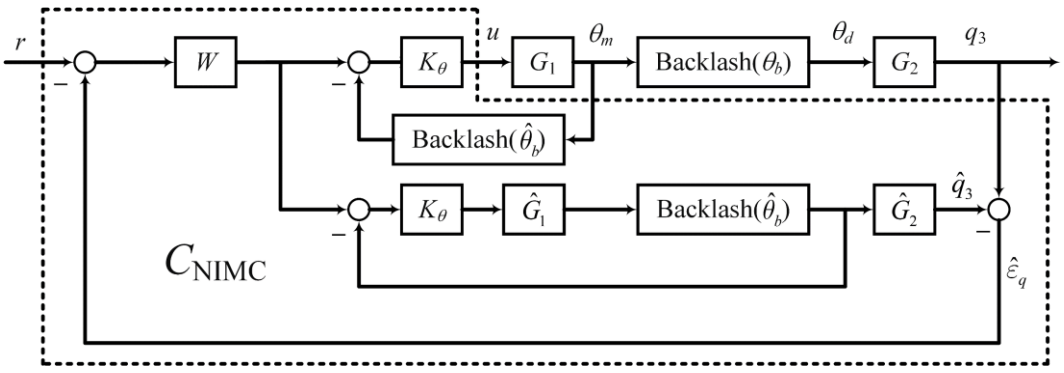

Figure 9: Block diagram of the nonlinear internal model control (NIMC) controller's architecture. A sampled-data model of the backlash is added to the internal feedback loop to compensate for the lead screw backlash. θ_b and $\hat{\theta}_b$ denote the actual and estimated backlash gap angle, respectively.

The proposed structure of the NIMC controller is shown in Figure 9. The idea is to control the predicted lead screw's angle instead of the measured motor's angle. This is achieved by adding a backlash model to

the internal feedback. The modelled system used to obtain the predicted output, $\hat{q}_3$, is also updated to represent the backlash between the motor and lead screw. The Simulink simulation of section 3.2 was rerun with the proposed NIMC and the same backlash gap angle profile. The motor's angular velocity used as the input of the backlash is obtained by passing u via a sampled-data model of the system $sG_1(s)$.

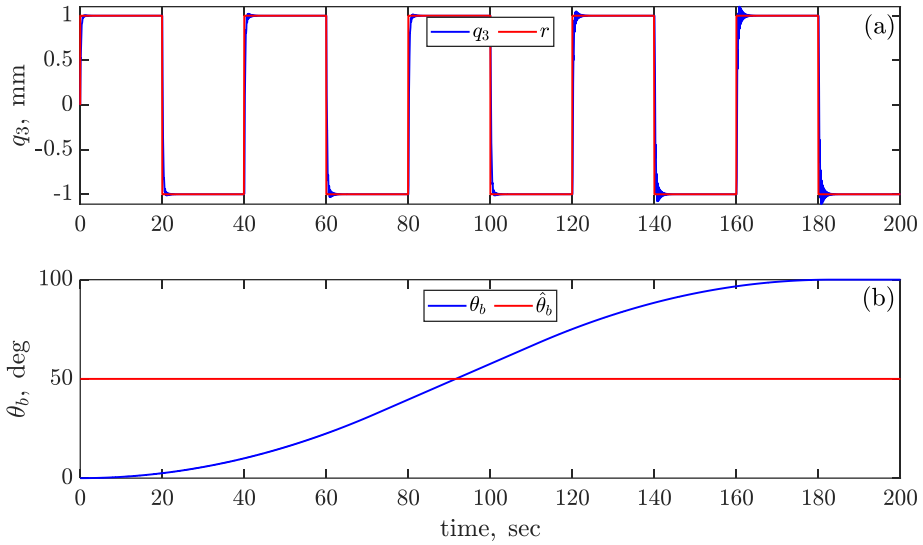

Figure 10: The time-varying backlash simulation results with the NIMC controller. The reference and output signals (a) and the actual and estimated backlash gap angles (b) versus time.

Figure 10 shows the simulation results with an estimated backlash gap angle of 50 degrees. It can be seen that when the backlash gap angle estimation is almost exact, at times between 80-120 seconds, the transient behaviour is similar to the designed one. Also, when the actual backlash is relatively small, the estimation error has a negligible effect on the transient. However, when the actual backlash is larger than the estimated one, the overshoot and decaying oscillations are again present in the transient response. Therefore, it is desired to reconfigure the backlash estimation, which can be done by employing a digital twin of the system.

4 Digital Twin

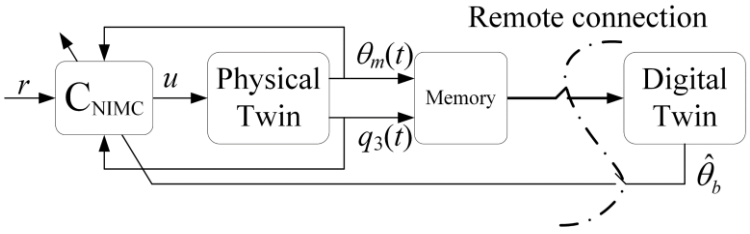

Figure 11: Block diagram of the architecture used to reconfigure the NIMC feedback controller using a digital twin.

A digital twin is used to estimate the backlash gap angle and to reconfigure the feedback controller. The digital twin is assumed to be implemented remotely and can communicate asynchronously with the feedback controller via a network, as shown in Figure 11. The measured system states, θ_m and q_3, are stored in local memory that is being sent to the digital twin when the reference signal value changes. The digital twin has pre-calibrated models that represent the different dynamical systems and can simulate the response of the nonlinear system at a faster than real-time rate, thus allowing to implement of a nonlinear identification technique to estimate the backlash gap angle.

4.1 Backlash gap estimation

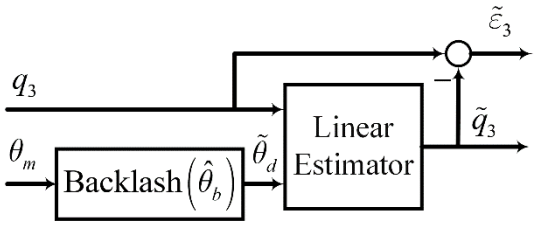

Figure 12: Mixed linear–nonlinear simulation used in the digital twin estimation of the backlash gap angle.

The backlash gap angle is estimated in the digital twin by minimising the residual mean square of an estimated error obtained from a numerical simulation that is realised using the digital twin at a high rate. A mixed linear-nonlinear approach is taken, as shown in Figure 12, to avoid the necessity to estimate the initial condition of the three DOF structure as part of the simulation.

By designing a linear state observer [12] as the linear estimator, it is guaranteed that if the estimated lead screw's angle, $\tilde{\theta}_d$, is exact than the estimated response, $\tilde{q}_3$, will converge with an exponential rate to the measured response, q_3. Therefore, the optimisation cost function is defined as:

$$\min_{\hat{\theta}_b, \theta_d(0)} \sum_{k=k_s}^{N-1} \left(\tilde{\varepsilon}_3(t_0 + kT_s)\right)^2 \tag{18}$$

where k_s is chosen based on the linear estimator settling time, and N is the number of measured points stored in the buffer.

The optimal solution of Eq. (18) can be obtained using many optimization methods [20]. In the current work, the unconstraint BFGS Quasi-Newton method with cubic line search was chosen to solve the optimization problem, which was realised using MATLAB's *fminunc*() function.

4.1.1 Numerical simulation of the digital twin reconfigurable controller

A combined Simulink and MATLAB simulation was used to validate the proposed reconfigurable NIMC approach. A buffer of 1000 samples of θ_m and q_3 was sent to the digital twin each time the reference signal changes its value (every 20 seconds). The backlash gap angle is estimated in the digital twin by minimizing Eq. (18). The linear estimator was designed to have a settling time of 0.25. This was done by designing an estimator with the following characteristic polynomial, $\chi_o(\lambda) = (\lambda + 40)^4$. The last 600 samples of the estimated output were then used in Eq. (18), i.e. $k_s = 401$. After the identification had converged to its optimal solution, and the backlash gap angle was estimated, the NIMC controller was reconfigure with the newly estimated backlash gap angle. A 4 seconds delay was added to compensate for the transmission and nonlinear optimization time.

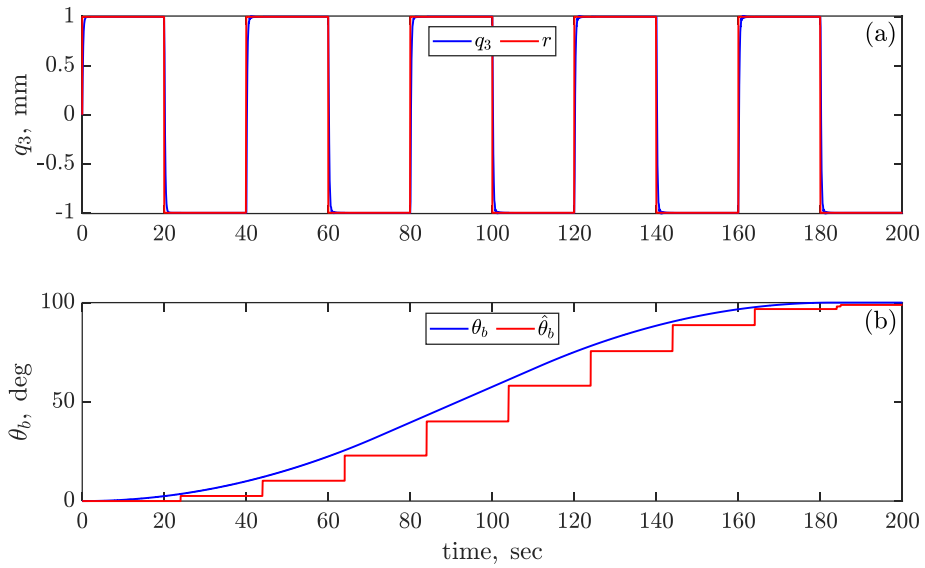

Figure 13: The time-varying backlash simulation results with the digital twin reconfigurable NIMC controller. The reference and output signals (a) and the actual and estimated backlash gap angles (b) versus time.

Figure 13 shows the simulation results when using the digital twin to estimate the backlash gap angle and reconfigure the NIMC controller. The introduction of the digital twin enables maintaining the desired transient behaviour, Figure 13(a), even though the reconfiguration of the controller is delayed by 4 seconds, as can be seen, best in Figure 13(b). Moreover, Figure 13(b) shows that the proposed backlash gap angle estimation is unbiased.

It is noted that the acceleration rate of the backlash gap angle profile here is unrealistic fast and is used only for simulation purposes. In reality, the backlash will change over weeks or months, and thus the short delay is insignificant. Moreover, the prediction error, already computed as part of the feedback loop by the controller, can be used to formulate a decision test, which dictates when the estimation and reconfiguration are needed.

4.2 Novelty index-based decision test

The novelty index proposed in the current work is the instantaneous amplitude of the dominant structure mode in the prediction error, $\hat{\varepsilon}_q$, as shown in Figure 9. This was chosen instead of the instantaneous amplitude of $\hat{\varepsilon}_q$, since the latter is susceptible to any measurement noise, although this is not modelled in these simulations. Also as noted in the simulations, the transient oscillations vibrate with the dominant mode damped frequency, ω_d.

The instantaneous amplitude of the first mode is obtained by using a frequency lock-in filter. The lock-in filter enables the extraction of the in-phase and quadrature components, such that the dominant mode analytic function is given by:

$$\hat{\eta}(t) = \hat{\eta}_r(t) - \mathrm{i}\hat{\eta}_i(t), \tag{19}$$

where the in-phase component $\hat{\eta}_r$, and quadrature component $\hat{\eta}_i$ are given by:

$$\hat{\eta}_r(t) = \mathrm{LPF}\big(2\hat{\varepsilon}_q(t)\cos\omega_d t\big), \tag{20}$$

$$\hat{\eta}_i(t) = \mathrm{LPF}\big(2\hat{\varepsilon}_q(t)\sin\omega_d t\big), \tag{21}$$

and LPF is a lowpass filter designed to have its cutoff frequency at $\omega_d/2$. The instantaneous modal amplitude is thus given by the absolute value of the analytic function, $\hat{\eta}(t)$.

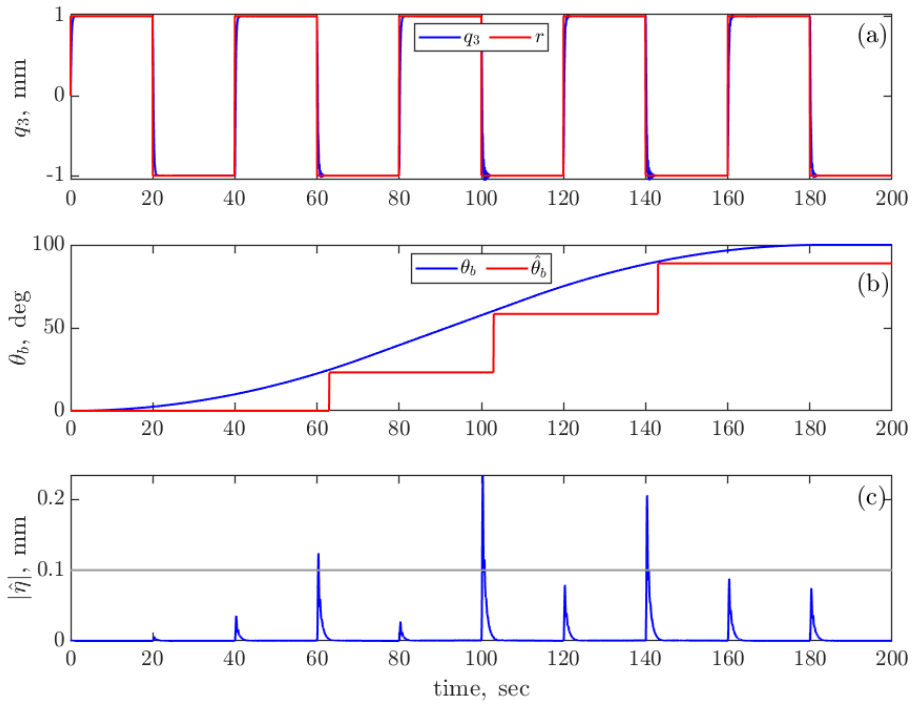

Figure 14: The time-varying backlash simulation results with novelty index-based decision test and a digital twin reconfigurable NIMC controller. The reference and output signals (a) and the actual and estimated backlash gap angles (b) versus time.

Figure 14 shows the simulation results when using the novelty index-based decision test combined with the digital twin. In the simulation, the novelty index was obtained using a numerically-controlled oscillator (NCO), a Cordic sin and cos generators and a third-order IIR LPF designed to have a stopband of 40dB at ω_d. An event was defined when the novelty index amplitude was larger than 0.1mm. In the case of an event, the conditions stored in the memory were sent to the digital twin, which estimated the backlash gap angle based on the nonlinear identification of Section 4.1 and reconfigured the NIMC feedback controller.

The novelty index used in the decision test is shown in Figure 14(c). Whenever the value of $|\eta|$ is larger than the predefined tolerance, indicated by the grey line, the backlash gap angle is estimated using the digital twin, as shown in Figure 14(b). The backlash model is now estimated only three times during the simulation, compared to the nine times in Section 4.1. Still, the transient behaviour of Figure 14(a) does not differ much from the one of Figure 13(a). Therefore, the advantage of using the novelty index-based decision test over updating the model each time the input signals changes is portrait. Moreover, designing several novelty indexes can allow reconfiguring different subsystems using the digital twin. For example, if we track the change of ω_d, we can decide if the dynamical model of the three DOF structure should be reestimated.

5 Conclusions

This paper presented the idea of utilising a digital twin in the position control of dynamical structures subject to time-varying nonlinear backlash. A linear IMC feedback controller with an internal feedback loop, was designed based on linear models of the system to stabilise it and to shape the transient system response. The effect of unmodelled time-varying backlash on the linear IMC design was investigated based on a numerical simulation. It was concluded that while the stability is kept, the transient behaviour is lost when the backlash becomes nonnegligible.

A nonlinear IMC, NIMC, architecture was proposed by including the backlash model in the controller. Based on simulative results, it was concluded that the desired transient behaviour is retained if the backlash model is exact. Therefore, it was suggested to estimate the backlash model using a remotely-based digital twin. The advantage of the digital twin used in the manner portraited here versus an adaptive controller that estimates the nonlinear model in the loop is that the resulting controller architecture when using the digital twin is simpler, and its implementation is more straightforward. Moreover, the digital twin can implement a nonlinear identification algorithm that requires simulating the system's response at a fast rate.

A mixed linear-nonlinear estimation method was designed to be used by the digital twin to estimate the backlash gap angle and, in turn, to reconfigure the NIMC feedback controller. The proposed methodology was validated numerically. It was shown that the backlash gap angle estimation is unbiased and that by utilizing the digital twin and reconfiguring the NIMC, the transient behaviour of the designed prefilter is kept.

A novelty index was derived based on the prediction error computed as part of the NIMC feedback loop. The novelty index-based decision test minimises the usage of the digital twin, thus ensuring that the digital twin will not be overflown. Additional advantages of using the proposed frequency lock-in filter for the novelty index are that it attenuates measurement noise and enables the formulation of additional novelty indexes associated with other subsystems.

Acknowledgements

The authors gratefully acknowledge the support of the UK Engineering and Physical Sciences Research Council (EPSRC) through the DigiTwin project (grant EP/R006768/1).

References

[1] M. Morari and E. Zafiriou, Robust process control. Prentice Hall, 1989.

[2] S. J. Elliott and T. J. Sutton, "Performance of feedforward and feedback systems for active control," IEEE Trans. Speech Audio Process., vol. 4, no. 3, pp. 214–223, 1996, doi: 10.1109/89.496217.

[3] S. J. Elliott, Signal processing for active control. Elsevier, 2001.

[4] C. Q. Economou, M. Morari, and B. O. Palsson, "Internal model control: extension to nonlinear system," Ind. Eng. Chem. Process Des. Dev., vol. 25, no. 2, pp. 403–411, 1986, doi: 10.1021/I200033A010.

[5] H. Qiuping and G. P. Rangaiah, "Adaptive internal model control of nonlinear processes," Chem. Eng. Sci., vol. 54, no. 9, pp. 1205–1220, 1999, doi: 10.1016/S0009-2509(98)00543-0.

[6] I. D. Landau, R. Lozano, M. M'Saad, and A. Karimi, Adaptive control: algorithms, analysis and applications. Springer Science & Business Media, 2011.

[7] D. J. Wagg, K. Worden, R. J. Barthorpe, and P. Gardner, "Digital twins: state-of-the-art and future directions for modeling and simulation in engineering dynamics applications," ASCE-ASME J Risk Uncert Engrg Sys Part B Mech Engrg, vol. 6, no. 3, Sep. 2020, doi: 10.1115/1.4046739.

[8] L. Ljung, System identification. Englewood Cliffs, NJ: Prentice Hall, 1999.

[9] S. Haykin, Neural networks: a comprehensive foundation. NJ: Prentice Hall, 1999.

[10] H. Ahmadian, J. E. Mottershead, and M. I. Friswell, "Regularisation methods for finite element model updating," Mech. Syst. Signal Process., vol. 12, no. 1, pp. 47–64, 1998, doi: 10.1006/mssp.1996.0133.

[11] M. Link, "Updating analytical models by using local and global parameters and relaxed optimisation requirements," Mech. Syst. Signal Process., vol. 12, no. 1, pp. 7–22, 1998, doi: 10.1006/mssp.1997.0131.

[12] K. J. Åström and R. M. Murray, Feedback systems. Princeton University Press, 2010.

[13] J. C. Doyle, B. A. Francis, and A. R. Tannenbaum, Feedback control theory. Courier Corporation, 2013.

[14] J. Vörös, "Modeling and identification of systems with backlash," Automatica, vol. 46, no. 2, pp. 369–374, Feb. 2010, doi: 10.1016/J.AUTOMATICA.2009.11.005.

[15] M. Nordin and P. O. Gutman, "Controlling mechanical systems with backlash—a survey," Automatica, vol. 38, no. 10, pp. 1633–1649, Oct. 2002, doi: 10.1016/S0005-1098(02)00047-X.

[16] G. Tao, X. Ma, and Y. Ling, "Optimal and nonlinear decoupling control of systems with sandwiched backlash," Automatica, vol. 37, no. 2, pp. 165–176, Feb. 2001, doi: 10.1016/S0005-1098(00)00153-9.

[17] K. Worden, "Structural fault detection using a novelty measure," J. Sound Vib., vol. 201, no. 1, pp. 85–101, Mar. 1997, doi: 10.1006/jsvi.1996.0747.

[18] M. Dal Borgo, P. Gardner, Y. Zhu, D. J. Wagg, S. K. Au, and S. Elliott, "On the development of a digital twin for the active vibration control of a three-storey structure," 2020.

[19] A. Varga, "Balancing free square-root algorithm for computing singular perturbation approximations," in Proceedings of the IEEE Conference on Decision and Control, 1991, vol. 2, pp. 1062–1065, doi: 10.1109/cdc.1991.261486.

[20] S. Boyd and L. Vandenberghe, Convex optimization. Cambridge University Press, 2004.